Proc. Natl. Acad. Sci. USA
Vol. 85, pp. 654–658, February 1988
Biochemistry

Selective visualization of gene structure with ultraviolet light

(photofootprinting/nucleosomes/H1 protein/transcription factor IIIA)

ZHOU WANG AND MICHAEL M. BECKER

Department of Biological Sciences, University of Pittsburgh, Pittsburgh, PA 15260

Communicated by James C. Wang, August 10, 1987

ABSTRACT **The ability of the ultraviolet (UV) "footprinting" technique to detect chromatin has been investigated *in vitro*. Two basic types of chromatin, a phased nucleosome and a phased nucleosome containing a phased H1 protein, have been reconstituted onto a cloned 5S ribosomal RNA gene from sea urchin. The histone–DNA interactions in each complex have been probed with exonuclease III, DNase I, dimethyl sulfate, and UV light. Whereas DNase I and exonuclease III readily detect interactions between histones and DNA, UV light and dimethyl sulfate do not. In contrast to histone–DNA interactions, we demonstrate that intimate sequence-specific contacts between the same sea urchin 5S DNA and the *Xenopus laevis* transcription factor IIIA (TFIIIA) are readily detected with UV light. Since the sensitivity of UV light for TFIIIA contacts is similar to its sensitivity for other regulatory protein–DNA contacts, these studies demonstrate the feasibility of using UV light to selectively visualize regulatory protein–DNA interactions *in vivo* with little or no interference from histone–DNA interactions.**

During development, gene expression is often regulated at the level of transcription. The study of the molecular mechanisms responsible for this regulation often involves introducing mutant and wild-type genes into appropriate recipient cells by injection, infection, or transfection techniques. Differences in gene expression resulting from mutation are then used to identify DNA sequences that are responsible for regulating transcription rates. More often than not, the sequences so identified are presumed to represent sites of critical protein–DNA interactions.

Presently, in higher organisms it is impossible to efficiently replace normal chromosomal copies of genes with mutant copies constructed *in vitro*. As a result, comparison of mutant and wild-type gene expression is limited to studies in which the normal regulatory constraints imposed on a gene by its integration into a specific site of a chromosome are removed (1).

Recently, we described the development of a "photofootprinting" technique that can detect, at high resolution, contacts between DNA and regulatory proteins (2). Most importantly, the photofootprinting technique can detect these interactions in whole cells (2, 3). Thus, by comparing the protein–DNA interactions of a gene in its active state to those in its inactive state, it is possible to identify DNA sequences that are responsible for regulating the expression of a gene in its native state.

One of our photofootprinting approaches uses ultraviolet (UV) photons to obtain high-resolution photographs of gene structure *in vivo*. After UV irradiation of whole cells, DNA is isolated from the cell before cellular repair of the DNA damage takes place. It is then purified and subjected to a series of chemical reactions that break its phosphate backbone only at the sites of photodamage. The DNA is then denatured, electrophoresed on a polyacrylamide sequencing gel, and the resulting strand breakage pattern is visualized by autoradiography using either indirect (4) or direct end-labeling techniques (2). Because protein contacts can inhibit or enhance UV photoproduct formation, differences in the strand-breakage patterns of protein-free and protein-bound DNA can be used to detect, at the base-pair (bp) level, protein–DNA contacts. Detection of protein–DNA contacts is believed to result from the ability of intimate protein contacts to prevent DNA from adopting a geometry necessary for the formation of a UV photoproduct. Since histone–DNA interactions characteristic of chromatin show little or no sequence specificity (5), we reasoned that their contacts with DNA would not be intimate enough to be detected by UV light. If true, UV light could be used to detect, *in vivo*, critical regulatory sequences in genes and their interactions with regulatory proteins during gene expression with little or no interference from histone–DNA interactions. The results of this paper demonstrate the feasibility of this approach.

MATERIALS AND METHODS

DNA Sample Preparation. A 270-bp *Eco*RI fragment of plasmid pLV405 containing the sea urchin 5S rRNA gene (6) was recloned into the *Eco*RI site of pHC624 (7) to yield plasmid pKB201. Typically, 20 mg of plasmid can be isolated per liter of *Escherichia coli*. Large amounts of the *Eco*RI fragment from pKB201 were purified by preparative polyacrylamide gel electrophoresis followed by electroelution. The protruding ends of the *Eco*RI fragment were labeled with [γ-^{32}P]ATP and T4 polynucleotide kinase followed by secondary restriction at the *Mnl* I or *Xmn* I site. A second 5S rRNA gene fragment was prepared from pKB201 by digestion with *Xmn* I and *Sal* I, filling in the *Sal* I end with Klenow fragment of DNA polymerase I and religating with T4 ligase to yield plasmid pKB221. The 5S genes end-labeled on the bottom strand were prepared by cutting pKB221 with *Eco*RI, labeling with [γ-^{32}P]ATP and polynucleotide kinase and secondary restriction with *Bgl* II.

Nucleosome Reconstitution. Calf thymus histones (Boehringer Mannheim) were first dissolved in 2 M NaCl/10 mM Tris·HCl, pH 8.0/1 mM EDTA/1 mM 2-mercaptoethanol at a histone concentration of 16 mg/ml. A 16-μl portion of this histone stock was added to 270 μl of TE buffer (10 mM Tris·HCl, pH 8/1 mM EDTA) and the diluted histone was slowly added to 170 μl of poly(glutamic acid) (Sigma; M_r, 60,000), which was dissolved in 0.1 M NaCl/10 mM Tris·HCl, pH 8/1 mm EDTA at a concentration of 12 mg/ml. The histone/poly(glutamic acid) mixture was gently shaken at 25°C for 2 hr followed by shaking at 4°C overnight. A 285-μl portion of the histone/poly(glutamic acid) mixture was slowly added to 15 μl of DNA solution containing 20 μg of *Eco*RI-cut pKB 201 containing a trace amount of ^{32}P-end-labeled DNA. The resulting mixture was shaken gently at

The publication costs of this article were defrayed in part by page charge payment. This article must therefore be hereby marked "*advertisement*" in accordance with 18 U.S.C. §1734 solely to indicate this fact.

Abbreviation: TFIIIA, transcription factor IIIA.

37°C for 2 hr and purified on a 5–20% sucrose gradient containing 0.1 M NaCl or 0.5 M NaCl and 10 mM Tris·HCl, pH 8/1 mM EDTA, at 4°C for 17 hr at 35,000 rpm on an SW 40 rotor. Fractions from the gradient were collected in bovine serum albumin-coated tubes, bovine serum albumin was added to a final concentration of 1 mg/ml, and histone–DNA complexes were localized by scintillation counting.

Nuclease Digestion and Dimethyl Sulfate Treatment of Nucleosomes. Nucleosome complexes isolated from the sucrose gradient were used directly by adding 5 μg of linear pHC624 (dimethyl sulfate) and adjusting the solution to a final concentration of 3 mM $CaCl_2$/10 mM $MgCl_2$ (DNase I) or 10 mM $MgCl_2$ (exonuclease III). DNase I (Sigma) digestions were at 37°C for 2 min with the indicated amounts of enzyme. Exonuclease III digestion was at 37°C using 0.03 unit of *Exo* III per μl for the indicated times. Alkylation by dimethyl sulfate was carried out at 20°C for the indicated times at a final dimethyl sulfate concentration of 0.6% (vol/vol).

UV Footprinting Analysis. Samples were irradiated with a 1000-W Hg/Xe lamp (Photon Technology, Princeton, NJ, PTI model A5000). Before impinging on the sample, the light was filtered through a water filter (PT102-A002) and a secondary focusing lens (PT102-AS002). When filtered UV light was used for analysis, a 270-nm narrow-band interference filter (Oriel 53355) was placed in front of the sample. Chemical cleavage of photoproducts was carried out as described (2) except that the $NaBH_4$ reduction reaction was stopped with 250 μl of 0.4 M NaOAc/HaAc, pH 5.0.

DNase I and UV Footprinting Analysis of the TFIIIA Complex. Unlabeled RI fragment (0.15 μg) from pKB201 containing a trace of the same fragment ^{32}P-end-labeled on the lower strand was incubated at 25°C for 30 min with the indicated amounts of *Xenopus laevis* TFIIIA protein (12).

RESULTS AND DISCUSSION

To examine whether histone–DNA interactions in chromatin can be detected with the UV footprinting technique, we have utilized and extended the nucleosome reconstitution system of Simpson and Stafford (6). Under appropriate conditions, reconstitution of highly purified chicken erythrocyte nucleosomal histones onto a 270-bp cloned fragment of a sea urchin 5S rRNA gene results in the formation of a highly phased nucleosome. In the phased nucleosome, sequence elements of the 5S gene uniquely position the nucleosome over the gene. We have repeated these reconstitution experiments with the 5S gene utilizing commercially available calf thymus histones containing the H2A, H2B, H3, and H4 nucleosomal proteins as well as the H1 protein. After reconstitution in the presence of polyglutamic acid, the histone–DNA mixture was split into two samples. One sample was layered onto a sucrose gradient containing 0.1 M NaCl to allow H1 binding, while the other aliquot was layered on a 0.5 M NaCl sucrose gradient to inhibit H1 binding (8). Under conditions of low salt in which H1 binds, reconstitution results in the formation of two histone–DNA complexes (Fig. 1 *A* and *B*). We have used DNase I digestion to probe the identity of these histone–DNA complexes. The DNase I digestion pattern of the slower-sedimenting complex shows strong protection every 10 bp, demonstrating the formation of a highly phased nucleosome (Fig. 2*A*). Indeed, the observed DNase I pattern is identical to the pattern previously obtained by Simpson and Stafford (6) using chicken nucleosomal histones and the same 5S gene. DNase I analysis of the second faster-sedimenting complex reveals that it contains the same phased nucleosome as the slower-sedimenting species as well as a highly phased H1 protein (Fig. 2*A*). The phasing of the nucleosome in this complex is unaltered by the binding of H1, and reconstitution experiments with purified H1 demonstrate that H1 binding to the 5S gene is dependent on the binding of the adjacent nucleosome (results not shown). Under high-salt conditions in which the H1 protein does not bind, reconstitution results in the formation of only one histone–DNA complex (Fig. 1*C*). DNase I digestion analysis of this complex reveals that it is identical to the slowly sedimenting phased nucleosome formed at lower salt concentration that lacks an H1 protein (results not shown).

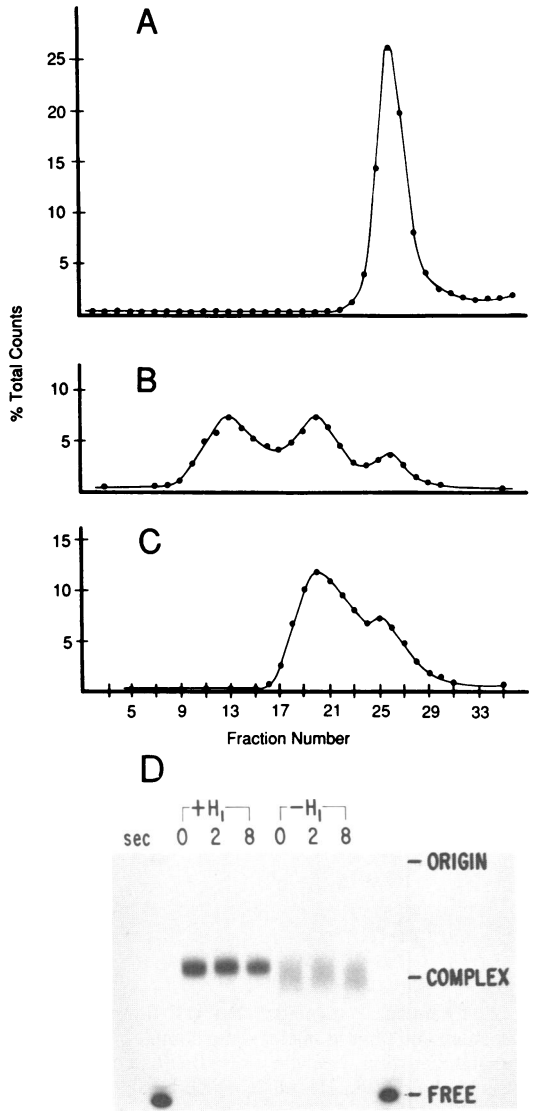

FIG. 1. Reconstitution of a phased sea urchin 5S rRNA gene with calf thymus histones. (*A*) Sucrose gradient profile of the 270-bp 5S gene in the absence of histone. Sucrose gradient profile of the 5S gene reconstituted with calf thymus histones under conditions of 0.1 M NaCl (*B*) or 0.5 M NaCl (*C*). (*D*) Low ionic strength polyacrylamide gel analysis of the phased H1–nucleosome and nucleosome complex isolated from the gradient in *B*, which has been irradiated with 0, 2, or 8 sec of broad-band light.

To examine the sensitivity of UV light to both nucleosome–DNA and H1–DNA contacts, we have probed exclusively the fast-sedimenting low-salt phased H1–nucleosome complex since it contains, in addition to H1, the same phased nucleosome as the slow-sedimenting low- and high-salt complexes. The phased H1–nucleosome complex was irradiated with broad-band light emitted from a mercury/xenon lamp, which emits both UV and visible light. Only the UV light component damages DNA since the same photoproducts result when this light is passed through a filter that only transmits at 270 nm (results not shown). When irradiated with broad-band light, analysis of the resulting photo-

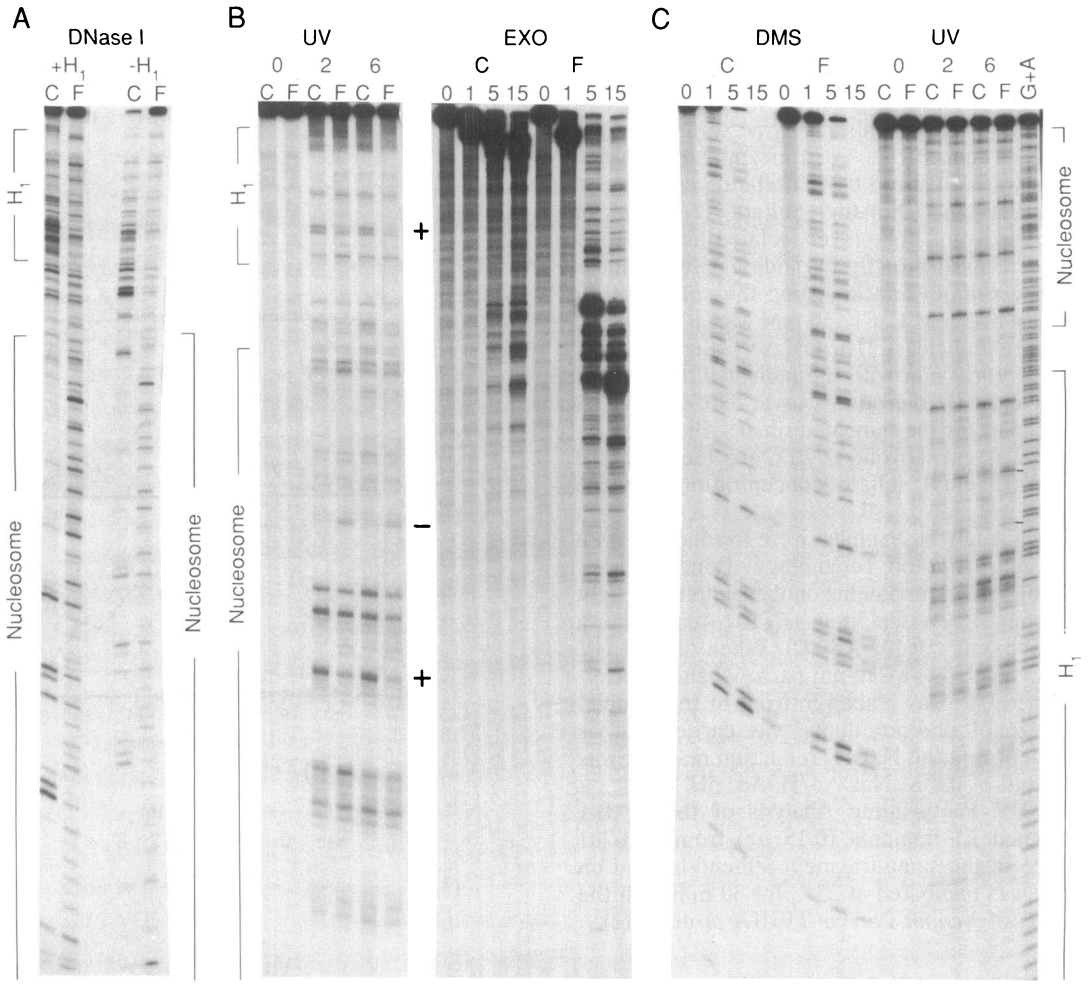

FIG. 2. Chemical, enzymatic, and UV footprinting analysis of phased nucleosome complexes. (*A*) DNase I analysis of the phased H1–nucleosome and phased nucleosome complex isolated from the gradient in Fig. 1*B*. The 5S gene was uniquely end-labeled with ^{32}P on the top strand and digestion was with either 0.6 (C; complex) or 0.06 (F; free) unit of DNase I per ml. (*B*) UV photofootprinting and exonuclease III analysis of the phased H1–nucleosome complex end-labeled with ^{32}P on the top strand. (*C*) Dimethyl sulfate (DMS) alkylation and UV photofootprinting analysis of the 5S gene uniquely end-labeled with ^{32}P on the lower strand.

products on sequencing gels demonstrates that the phased H1–nucleosome complex only weakly protects DNA from UV damage at a few scattered sites (Fig. 2*B*). In contrast, the phased H1–nucleosome complex strongly protects the 5S gene from DNase I or exonuclease III digestion (Fig. 2 *A* and *B*). We have also analyzed the formation of UV-induced photoproducts on the lower strand of the phase H1–nucleosome complex. As shown in Fig. 2*C*, phased H1–nucleosome contacts on the lower strand, like the upper strand, only weakly protect DNA from UV damage at a few scattered sites. In contrast, the phased H1–nucleosome complex strongly protects the lower strand from DNase I digestion (results not shown).

The results presented in Fig. 2 demonstrate that UV light only weakly detects phased H1 or phased nucleosome contacts. Unphased H1–nucleosome contacts are expected to show even lower sensitivity to detection by UV light. We believe that the inability of UV light to detect histone–DNA interactions is due to the failure of histone proteins to make sufficient intimate contact with the DNA bases so as to alter their ability to adopt a geometry necessary for UV photoproduct formation. In support of this hypothesis we find that the very small alkylating agent dimethyl sulfate, which is believed to detect only intimate contacts between DNA and protein (10), also fails to detect phased H1–nucleosome interactions (Fig. 2*C*).

Although it appears likely that histone–DNA interactions are not intimate enough to be detected by UV light, we have assumed that during irradiation histone–DNA contacts are not dissociated by UV light. To address this issue, we have compared the binding of phased nucleosomes, as well as phased H1–nucleosome complexes before and after irradiation with UV light. As shown in Fig. 1*D*, irradiation of the phased nucleosome or phased nucleosome–H1 complex under the conditions of our experiments does not induce H1 or nucleosome dissociation.

Chromatin Versus Regulatory Proteins. In contrast to our measurements with chromatin, we have previously demonstrated that intimate contacts between *lac* repressor and the *lac* operon strongly (20-fold or greater) inhibit the formation of UV photoproducts (2). Similar results have been obtained with another sequence-specific binding protein, the *Eco*RI endonuclease (M.M.B., D. Lesser, M. Kurpewski, A. Baranger, and L. Jen-Jacobson, unpublished results). To examine further the possibility that UV light only detects intimate contacts between DNA and protein, we have examined the sensitivity of our UV footprinting technique to interactions between DNA and *X. laevis* transcription factor TFIIIA. We chose to investigate this eukaryotic protein since previous measurements have demonstrated that the TFIIIA protein binds tightly and sequence specifically to sequences within *Xenopus* 5S rRNA genes (11, 12). Since our sea urchin 5S rRNA gene is very homologous to *Xenopus* 5S rRNA genes, we investigated the binding of the *Xenopus* TFIIIA protein to the sea urchin 5S DNA. If the *Xenopus* factor bound to our fragment, it would be possible

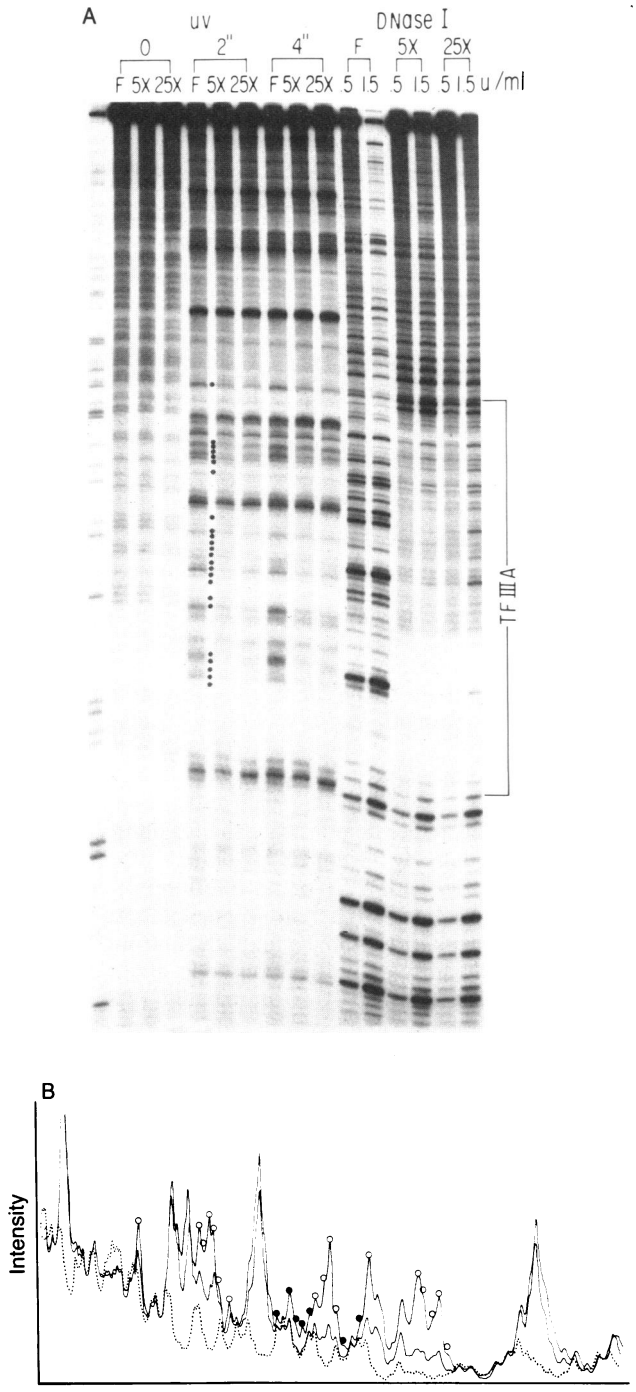

FIG. 3. DNase I and UV footprinting analysis of the *X. laevis* TFIIIA–5S sea urchin gene complex. (*A*) DNA in the absence of TFIIIA (F; free) or in the presence of 5 M excess (×5) or 25 M excess (×25) TFIIIA is irradiated with 0, 2, or 4 sec of 270-nm light (42×10^{-3} W/cm^2) or digested with DNase I. Sites of altered UV photoproduct formation due to TFIIIA binding are denoted by solid circles. The drop in intensity observed midway in both UV and DNase I footprints is due to a salt gradient moving through the gel. The 5S gene was uniquely end-labeled with ^{32}P on the lower strand in all cases. (*B*) Densitometric scans of the TFIIIA–5S sea urchin gene complex probed with UV light. The upper trace is DNA irradiated in the absence of TFIIIA, while the middle trace is DNA irradiated in the presence of TFIIIA. The lower (dotted) trace shows the strand breakage of unirradiated DNA, which has been carried through the same chemical reactions used to induce strand breakage at UV photoproducts in the upper two traces. Circles correspond to protected bases denoted on the autoradiograph in *A*. When filled in, these circles denote strongly protected bases. Irradiation was for 2 sec and the 5S gene was uniquely end-labeled with ^{32}P on the lower strand.

to directly compare, over the same DNA sequence, the sensitivity of UV light for histone–DNA interactions versus the intimate sequence-specific contacts of a transcription factor. Our preliminary experiments revealed that although the *Xenopus* TFIIIA factor binds to its homologous binding site in the sea urchin 5S gene, the interaction is readily disrupted by weak digestion with DNase I treatment, with dimethyl sulfate, or irradiation with broad-band light (results not shown). To avoid these problems, we first probed the sea urchin TFIIIA interaction with small amounts of DNase I. As shown in Fig. 3*A*, under these conditions we were able to obtain a very strong TFIIIA DNase I footprint. To probe this complex with UV light, we passed the broad-band light from our lamp through a 270-nm filter to remove long UV wavelengths, which we felt were dissociating the complex. Under these conditions, we were able to detect the TFIIIA complex with UV light. As shown in Fig. 3*A*, the binding region detected with UV light closely matches the binding site detected with DNase I. When compared to previous measurements, the binding site detected by UV light and DNase I is virtually identical to the homologous site detected in *Xenopus* (9, 11, 12).

To compare the sensitivity of UV light for the sequence-specific contacts of the TFIIIA factor versus its sensitivity for histone–DNA interactions, we have quantitated by microdensitometry the autoradiographs of Figs. 2 and 3*A*. A densitometric scan of the TFIIIA UV footprint is shown in

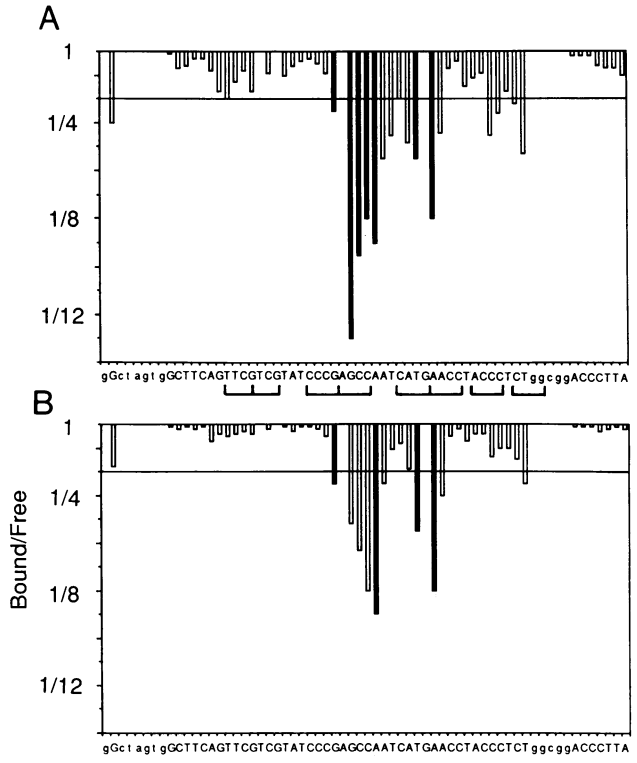

FIG. 4. Quantitation of the UV footprinting results of the TFIIIA–5S gene complex. The autoradiograph in Fig. 3*A* was quantitated by microdensitometry. Inhibition of photoproduct formation is expressed as the bound/free ratio (see text for details of this calculation). The TFIIIA–5S gene complex was irradiated for 2 sec with 5 M excess TFIIIA (*A*), or 25 M excess TFIIIA (*B*). The weaker footprint observed for 25 M excess TFIIIA complex is consistent with the weaker DNase I footprint observed for this complex (see Fig. 3*A*). Previously proposed Zn-binding fingers (9) are denoted by brackets. The 5S gene was end-labeled with ^{32}P on the lower strand. Solid regions of the histogram denote strongly protected bases (see Fig. 3*B*) whose protection is equal to or greater than the indicated ratio. The horizontal line at bound/free = 1/3 denotes the maximum protection observed on either strand for the phased H1 nucleosome.

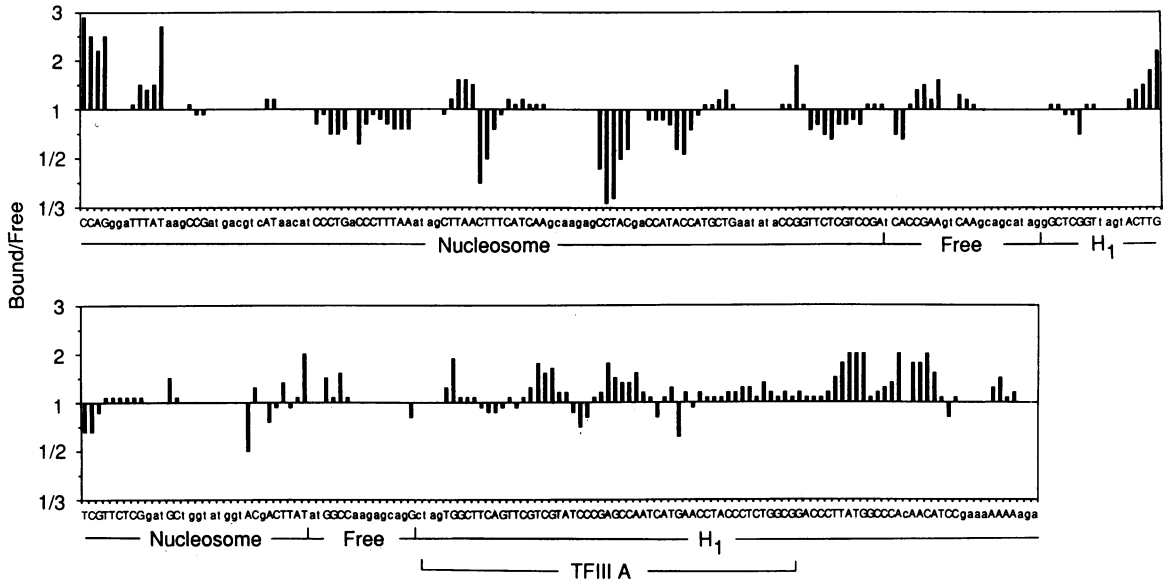

FIG. 5. Quantitation of the UV footprinting results of the phased H1–nucleosome complex. The autoradiograph in Fig. 2 was quantitated by microdensitometry. Inhibition or enhancement of photoproduct formation is expressed as the bound/free ratio as in Fig. 4.

Fig. 3*B*. We express detection of protein binding by UV light as a bound/free ratio, where bound is the intensity of photoproduct formation at a particular base in the presence of bound protein minus the intensity of the same base observed in the absence of light. This latter correction is necessary since the chemical reactions used to induce strand breakage at the sites of photodamage also induce some strand breakage in unirradiated DNA. A similar calculation in the absence of protein binding yields the free quantity. The location of each photoproduct within the sequence is determined by noting that the chemistry used to induce strand breakage at the sites of photoproduct formation is expected to induce breakage at the 3′ phosphate of the damaged base (13). Thus, when compared to strand breakage of the same base induced by the sequencing chemistry of Maxam and Gilbert (14), our 5′-end-labeled DNA should migrate as if it were 1 bp longer. This behavior is clearly exhibited by unirradiated DNA that has been subjected to the same reactions used to induce strand breakage of photoreacted DNA. As shown in Fig. 2*C* and 3*A*, the acidic aniline used to induce cleavage of photoreacted DNA induces a small amount of depurination in unirradiated DNA, yielding a strand-breakage pattern identical but displaced 1 base relative to the depurination chemistry of Maxam and Gilbert. Although the possibility exists that the DNA backbone may not be cleaved exactly at the site of the photodamaged base by our chemistry, results with an alternative method of photoproduct detection argue against this possibility. We have developed a primer-extension method to detect UV photoproduct formation (G. Grossmann, K. Becherer, and M.M.B., unpublished results). After UV irradiation, DNA is denatured and hybridized to a small complementary ^{32}P-labeled primer. The Klenow fragment of DNA polymerase I is then allowed to extend the primer. We find that the photoproducts detected in this manner are the same whether or not our chemistry is used to induce strand breaks in the DNA before extension by the Klenow fragment. Thus, it is unlikely that our chemistry induces strand breakage at bases other than those directly damaged by UV light.

As summarized in Fig. 4, binding of the *Xenopus* TFIIIA factor to the 5S sea urchin gene strongly inhibits the formation of UV photoproducts. Only those photoproducts that lie within the known binding of the TFIIIA factor show inhibition of UV photoreactivity. In contrast to TFIIIA contacts, histone–DNA contacts to the same DNA only weakly inhibit (or enhance) the formation of UV photoproducts (Fig. 5).

CONCLUSIONS

The results of this paper demonstrate the feasibility of using UV light to selectively visualize regulatory protein–DNA interactions *in vivo* with little or no interference from histone–DNA interactions. Whereas sequence-specific contacts between regulatory proteins and DNA strongly inhibit or enhance (3) the formation of UV photoproducts, histone–DNA interactions do not. It is anticipated that the UV footprinting technique will make it possible to detect *in vivo*, and within the chromosome, critical regulatory sequences and their interactions with regulatory proteins during gene expression.

We wish to thank Darrell Stafford for plasmid pLV405, Donald Brown for the *Xenopus* TFIIIA factor, and Kathleen Becherer for excellent technical assistance. This work was supported in part by funds from the American Cancer Society (IN-58W), the Health Research and Science Foundation (BB-33), the March of Dimes (5-554), and by National Science Foundation Grant DMB 02530 to M.B.B. M.B.B. is a recipient of a Basil O'Connor Starter Scholar Award (5-554) from the March of Dimes.

1. Lewis, E. B. (1950) *Adv. Genet.* **3**, 73–115.
2. Becker, M. M. & Wang, J. C. (1984) *Nature (London)* **309**, 682–687.
3. Selleck, S. B. & Majors, J. (1987) *Nature (London)* **325**, 173–177.
4. Church, G. M. & Gilbert, W. (1984) *Proc. Natl. Acad. Sci. USA* **81**, 1991–1995.
5. Purnel, A. & Kornberg, R. (1982) *J. Mol. Biol.* **154**, 515–523.
6. Simpson, R. T. & Stafford, D. W. (1983) *Proc. Natl. Acad. Sci. USA* **80**, 51–55.
7. Boros, I., Posfai, G. & Venetianer, P. (1984) *Gene* **30**, 257–260.
8. Bolund, L. A. & Johns, E. W. (1973) *Eur. J. Biochem.* **35**, 546–553.
9. Fairall, L., Rhodes, D. & Klug, A. (1986) *J. Mol. Biol.* **192**, 577–591.
10. Gilbert, W., Maxam, A. & Mirzabeka, A. (1976) in *Control of Ribosome Synthesis*, eds. Kjeldgaard, N. C. & Maaloe, O. (Munksgaard, Copenhagen), pp. 139–148.
11. Engelke, D. R., Ng, S.-Y., Shastry, B. S. & Roeder, R. G. (1980) *Cell* **19**, 717–728.
12. Sakonju, S. & Brown, D. D. (1982) *Cell* **31**, 395–405.
13. Wintermeyer, W. & Zachau, H. G. (1982) *FEBS Lett.* **58**, 306–309.
14. Maxam, A. M. & Gilbert, W. (1980) *Methods Enzymol.* **65**, 497–560.